

A Single-Crystalline, Epitaxial SrTiO₃ Thin-Film Transistor

Kosuke Uchida¹, Akira Yoshikawa¹, Kunihito Koumoto¹, Takeharu Kato², Yuichi Ikuhara^{2,3}, and Hiromichi Ohta^{1,4,a)}

¹*Graduate School of Engineering, Nagoya University, Chikusa, Nagoya 464-8603, Japan*

²*Japan Fine Ceramics Center, Mutsuno, Atsuta, Nagoya 456-8587, Japan*

³*Institute of Engineering Innovation, The University of Tokyo, Bunkyo, Tokyo 113-8656, Japan*

⁴*PRESTO, Japan Science and Technology Agency, Honcho, Kawaguchi 332-0012, Japan*

^{a)}Correspondence should be addressed H.O. (h-ohta@apchem.nagoya-u.ac.jp)

PACS: 81.15.Fg Pulsed laser ablation deposition, 73.61.Le Other inorganic semiconductors, 85.30.Tv Field effect devices, 77.55.D- High-permittivity gate dielectric films

Abstract

We report herein fabrication and characterization of a thin-film transistor (TFT) using single-crystalline, epitaxial SrTiO₃ film, which was grown by a pulsed laser deposition technique followed by the thermal annealing treatment in an oxygen atmosphere. Although TFTs on the polycrystalline epitaxial SrTiO₃ films (as-deposited) exhibited poor transistor characteristics, the annealed single-crystalline SrTiO₃ TFT exhibits transistor characteristics comparable with those of bulk single-crystal SrTiO₃ FET: an on/off current ratio $>10^5$, sub-threshold swing $\sim 2.1 \text{ Vdecade}^{-1}$, and field-effect mobility $\sim 0.8 \text{ cm}^2\text{V}^{-1}\text{s}^{-1}$. This demonstrates the effectiveness of the appropriate thermal annealing treatment of epitaxial SrTiO₃ films.

Strontium titanate (SrTiO₃, cubic perovskite, $Pm3m$, lattice constant $a = 3.905 \text{ \AA}$) is known as a band insulator with a wide bandgap of $\sim 3.2 \text{ eV}$. SrTiO₃ has attracted growing attention for the next generation of *oxide electronics*¹ because it exhibits several unique properties. Charge carrier concentration of SrTiO₃ can be easily varied from insulating to metallic ($n_{3D} \sim 10^{21} \text{ cm}^{-3}$) by appropriate substitution doping, such as Nb⁵⁺ (Ti⁴⁺ site) or La³⁺ (Sr²⁺ site).^{2, 3} In addition, SrTiO₃ exhibits extremely high Hall mobility of $> 10^4 \text{ cm}^2\text{V}^{-1}\text{s}^{-1}$ at low temperatures.⁴ High-quality single crystals of SrTiO₃, which is commercially available, are widely used in the heteroepitaxial film growth of several perovskite oxides, such as high- T_c cuprates and manganates. The recent finding of high-density two-dimensional electron gas (2DEG) by Ohtomo and Hwang,⁵ confined within an extremely thin layer at the LaAlO₃/SrTiO₃ heterointerface, further accelerates the motivation for the realization of SrTiO₃-based electronic devices.

One of the most important devices to prove the viability of SrTiO₃ is the field-effect transistor (FET). A number of SrTiO₃-based FETs have been reported to date, using bulk single crystals of SrTiO₃.⁶⁻¹¹ Very recently, Ueno and co-workers observed a superconducting transition ($T_c \sim 0.4 \text{ K}$) of electrostatically accumulated 2D electron channel (sheet charge concentration $n_{2D} = 1-10 \times 10^{13} \text{ cm}^{-2}$) in a SrTiO₃ single crystal with an electric double layer gating technique.¹² They modulated the mean depth of carrier distribution (channel thickness) down from 16 to 3 nm, which corresponds to only 7-40 unit cells of SrTiO₃. This shows that a SrTiO₃-based thin-film transistor (TFT) is appropriate for practical 2D electron channel applications, since channel thickness of the TFT can be reduced further. However, SrTiO₃-based TFTs have not yet been reported.

In order to develop a SrTiO₃ TFT, we first tried to fabricate several top-gate TFTs by using $\sim 60\text{-nm}$ thick epitaxial SrTiO₃ films, which were grown by pulsed laser deposition (PLD, KrF excimer laser, $\sim 0.5 \text{ Jcm}^{-1}\text{pulse}^{-1}$, 20 ns, 5 Hz) on the (001) face of [(LaAlO₃)_{0.3}(Sr₂AlTaO₆)_{0.7}] (LSAT) substrates at 900°C in an oxygen pressure of $5 \times 10^{-4} \text{ Pa}$.

We used amorphous $12\text{CaO}\cdot 7\text{Al}_2\text{O}_3$ (*a*-C12A7, permittivity $\epsilon_r = 12$) as the gate insulator because single crystal SrTiO_3 -FETs with such gates exhibit nearly ideal transistor characteristics (Ref. 11).

The resultant TFTs, however, exhibited normally-ON-type behavior with poor transistor characteristics. The on-off current ratio and sub-threshold swing S-factor were $<10^2$ and ~ 20 Vdecade^{-1} , respectively, which were worse than those of single-crystal SrTiO_3 FET,¹¹ most likely due to the high density of oxygen vacancies and/or charge traps in the SrTiO_3 film (data not shown). Furthermore, the surface of the films was composed of fine grains (~ 30 nm in diameter), although the stepped-and-terraced LSAT surface was also observed in atomic force microscope (AFM) images [Fig. 1(a)], indicating that layer-by-layer growth has occurred. In summary, the as-deposited SrTiO_3 films were oxygen-deficient, polycrystalline and epitaxial.

To overcome these problems, the as-deposited SrTiO_3 films were annealed at 900°C in an oxygen pressure of ~ 1 Pa. We expected the polycrystalline film to be converted into a single crystal during thermal annealing via solid-phase diffusion. We obtained single-crystalline, epitaxial SrTiO_3 films with stepped-and-terraced surfaces. The resultant TFT exhibited characteristics comparable with those of a single-crystal SrTiO_3 FET: on/off current ratio greater than 10^5 , S-factor ~ 2.1 Vdecade^{-1} , and field-effect mobility $\mu_{\text{FE}} \sim 0.8$ $\text{cm}^2\text{V}^{-1}\text{s}^{-1}$. Here we report the fabrication and characterization of a SrTiO_3 TFT using a single-crystalline, epitaxial film of SrTiO_3 .

First, polycrystalline, epitaxial SrTiO_3 films (thickness: ~ 60 nm) were grown on the (001) face of LSAT substrates by PLD as described above. After the film growth, pure O_2 gas (1 Pa) was introduced into the PLD chamber to fill the oxygen deficiency of the SrTiO_3 film. The film was then annealed at 900°C for 30 min in an oxygen atmosphere and then cooled to room temperature. Figure 1(b) shows a topographic AFM image of the annealed film surface. The image shows atomically flat terraces and steps, which correspond to unit cell height of SrTiO_3 (0.3905 nm), without any grain boundaries. Crystallographic orientation and thickness of the

films were evaluated by high-resolution X-ray diffraction (HRXRD, ATX-G, Rigaku Co.) using monochromated Cu $K\alpha_1$ radiation. Only the intense diffraction peak of 002 SrTiO₃ is observed, together with 002 LSAT in the out of plane Bragg diffraction pattern [Fig. 1(c)]. Pendellösung fringes, which indicate that the thickness of SrTiO₃ is 60 nm, are clearly seen around the 002 SrTiO₃ [inset of Fig. 1(c)]. From these results, we concluded that the polycrystalline epitaxial as-deposited film was converted into a single crystal by this thermal annealing.

We subsequently fabricated a top-gate TFT using single crystalline SrTiO₃ epitaxial film as shown in Fig. 2. First, 20-nm-thick, metallic Ti films were deposited for use as the source and drain electrodes. The deposition was performed through a stencil mask by electron beam (EB) evaporation (base pressure $\sim 10^{-4}$ Pa, no substrate heating). Second, 160-nm-thick *a*-C12A7 film was deposited through a stencil mask by PLD ($\sim 3 \text{ J cm}^{-2} \text{ pulse}^{-1}$, oxygen pressure ~ 0.1 Pa) using dense polycrystalline C12A7 ceramic as a target. Finally, a gate electrode – a 20-nm-thick metallic Ti film – was deposited through a stencil mask by EB evaporation. The resultant TFT was annealed at 200°C in air atmosphere to reduce the oxygen defects generated during the *a*-C12A7 deposition.

Figure 3 shows the cross sectional high-resolution transmission electron microscope (HRTEM, TOPCON EM-002B with an accelerating voltage of 200 kV) image of the Ti/*a*-C12A7/SrTiO₃/LSAT interfacial region. We clearly observe a multilayer structure. The thicknesses of Ti, *a*-C12A7 and SrTiO₃ are 20, 160 and 60 nm, respectively. The heterointerface between *a*-C12A7/SrTiO₃ is abrupt. While *a*-C12A7 is featureless, the crystal structure of the SrTiO₃ film is clearly observable. A nano-beam diffraction patterns corresponding to *a*-C12A7 indicates that *a*-C12A7 is a glass film.

Transistor characteristics of the resultant SrTiO₃ TFT were measured with a semiconductor device analyzer (B1500A, Agilent Technologies) at room temperature. The channel width (W) and the channel length (L) of the TFT were 400 and 200 μm , respectively. Figure 4 shows typical (a) transfer and (b) output characteristics of the resultant TFT. Drain

current (I_d) of the FET increased as the gate voltage (V_g) increased, hence the channel was n -type, and electron carriers were accumulated by positive V_g [Fig. 4(a)]. We observed a rather large threshold gate voltage (V_{th}) of +6.5 V, obtained from a linear fit of an $I_d^{0.5}-V_g$ plot [inset of (a)], which corresponds to an electron trapping state density of $\sim 5 \times 10^{12} \text{ cm}^{-2}$. We also observed a clear pinch-off and current saturation in I_d [Fig. 4(b)], indicating that the operation of this TFT conformed to standard FET theory. The on/off current ratio, S-factor and V_{th} were $>10^5$, $\sim 2.1 \text{ Vdecade}^{-1}$ and +6.5 V, respectively. We calculated the sheet charge concentration (n_{xx}) and the field-effect mobility (μ_{FE}) of the SrTiO₃-TFTs. The n_{xx} values were obtained from $n_{xx} = C_i(V_g - V_{th})$, where C_i was the capacitance per unit area (67 nFcm^{-2}). The μ_{FE} values were obtained from $\mu_{FE} = g_m[(W/L)C_i \cdot V_d]^{-1}$, where g_m was transconductance $\partial I_d / \partial V_g$. The maximum μ_{FE} for this TFT was $\sim 0.8 \text{ cm}^2 \text{V}^{-1} \text{s}^{-1}$.

These values of on/off current ratio, S-factor, V_{th} and μ_{FE} are comparable to those of a single-crystal SrTiO₃ FET. The values for the as-deposited polycrystalline SrTiO₃-based TFT were significantly worse, demonstrating the effectiveness of appropriate thermal annealing treatment of epitaxial SrTiO₃ films.

In summary, we have fabricated the first thin-film transistor (TFT) which uses a single-crystalline epitaxial SrTiO₃ film. We found that polycrystalline epitaxial SrTiO₃ films can be converted into single crystals by thermal annealing. The resultant TFT exhibits transistor characteristics comparable to those of bulk single crystal SrTiO₃ FET: on/off current ratio $>10^5$, sub-threshold swing $\sim 2.1 \text{ Vdecade}^{-1}$, and field-effect mobility $\sim 0.8 \text{ cm}^2 \text{V}^{-1} \text{s}^{-1}$. Appropriate thermal annealing treatment of epitaxial SrTiO₃ films in an oxygen atmosphere is necessary to reduce the number of oxygen vacancies and create single-crystal structures.

A part of this work was financially supported by MEXT (Nano Materials Science for Atomic-scale Modification, 20047007).

References

- [1] R. Ramesh and D. G. Schlom, *Mater. Res. Soc. Bull.* **33**, 1006 (2008) and articles therein.
- [2] T. Okuda, K. Nakanishi, S. Miyasaka, and Y. Tokura, *Phys. Rev. B*, **63**, 113104 (2001).
- [3] S. Ohta, T. Nomura, H. Ohta, and K. Koumoto, *J. Appl. Phys.*, **97**, 034106 (2005).
- [4] O. N. Tufte and P. W. Chapman, *Phys. Rev.* **155**, 796 (1967).
- [5] A. Ohtomo and H. Y. Hwang, *Nature*. **427**, 423 (2004).
- [6] I. Pallecchi, G. Grassano, D. Marrié, L. Pellegrino, M. Putti, and A. S. Siri, *Appl. Phys. Lett.* **78**, 2244 (2001).
- [7] K. Ueno, I. H. Inoue, H. Akoh, M. Kawasaki, Y. Tokura, and H. Takagi, *Appl. Phys. Lett.* **83**, 1755 (2003).
- [8] K. Shibuya, T. Ohnishi, T. Uozumi, T. Sato, M. Lippmaa, M. Kawasaki, K. Nakajima, T. Chikyow, and H. Koinuma, *Appl. Phys. Lett.* **88**, 212116 (2006).
- [9] K. Shibuya, T. Ohnishi, M. Lippmaa, M. Kawasaki, and H. Koinuma, *Appl. Phys. Lett.* **85**, 425 (2004).
- [10] H. Nakamura, H. Takagi, I. H. Inoue, Y. Takahashi, T. Hasegawa, and Y. Tokura, *Appl. Phys. Lett.* **89**, 133504 (2006).
- [11] H. Ohta, Y. Masuoka, R. Asahi, T. Kato, Y. Ikuhara, K. Nomura, and H. Hosono, *Appl. Phys. Lett.* **95**, 113505 (2009).
- [12] K. Ueno, S. Nakamura, H. Shimotani, A. Ohtomo, N. Kimura, T. Nojima, H. Aoki, Y. Iwasa, and M. Kawasaki, *Nature Mater.* **7**, 855 (2008).

FIG. 1 (Color online) Topographic AFM images of SrTiO₃ epitaxial films [(a) as-deposited, (b) annealed in an oxygen atmosphere of 1 Pa]. (c) Out-of-plane XRD pattern of the SrTiO₃ epitaxial film. The inset shows Pendellösung fringes around the 002 diffraction peak of SrTiO₃.

FIG. 2 (Color online) The schematic device structure of a SrTiO₃ TFT. Ti films (20-nm-thick) are used as the source, drain and gate electrodes. A 160-nm-thick *a*-C12A7 film serves as the gate insulator. Channel length (L) and channel width (W) are 200 and 400 μm , respectively.

FIG. 3 (Color online) (a) Cross-sectional high-resolution transmission electron microscope image of the 160-nm-thick *a*-C12A7/SrTiO₃/LSAT heterointerface. (b) The magnified image around the *a*-C12A7/SrTiO₃ heterointerface. (c) Nano-beam diffraction pattern of *a*-C12A7 layer (upper) and selected area electron diffraction pattern of SrTiO₃ layer (lower).

FIG. 4 (Color online) (a) Typical transfer and (b) output characteristics of a TFT with a single-crystalline SrTiO₃ epitaxial film active layer, obtained by thermal annealing in an oxygen atmosphere. The inset of (a) shows $I_d^{0.5}-V_g$ plot of this TFT.

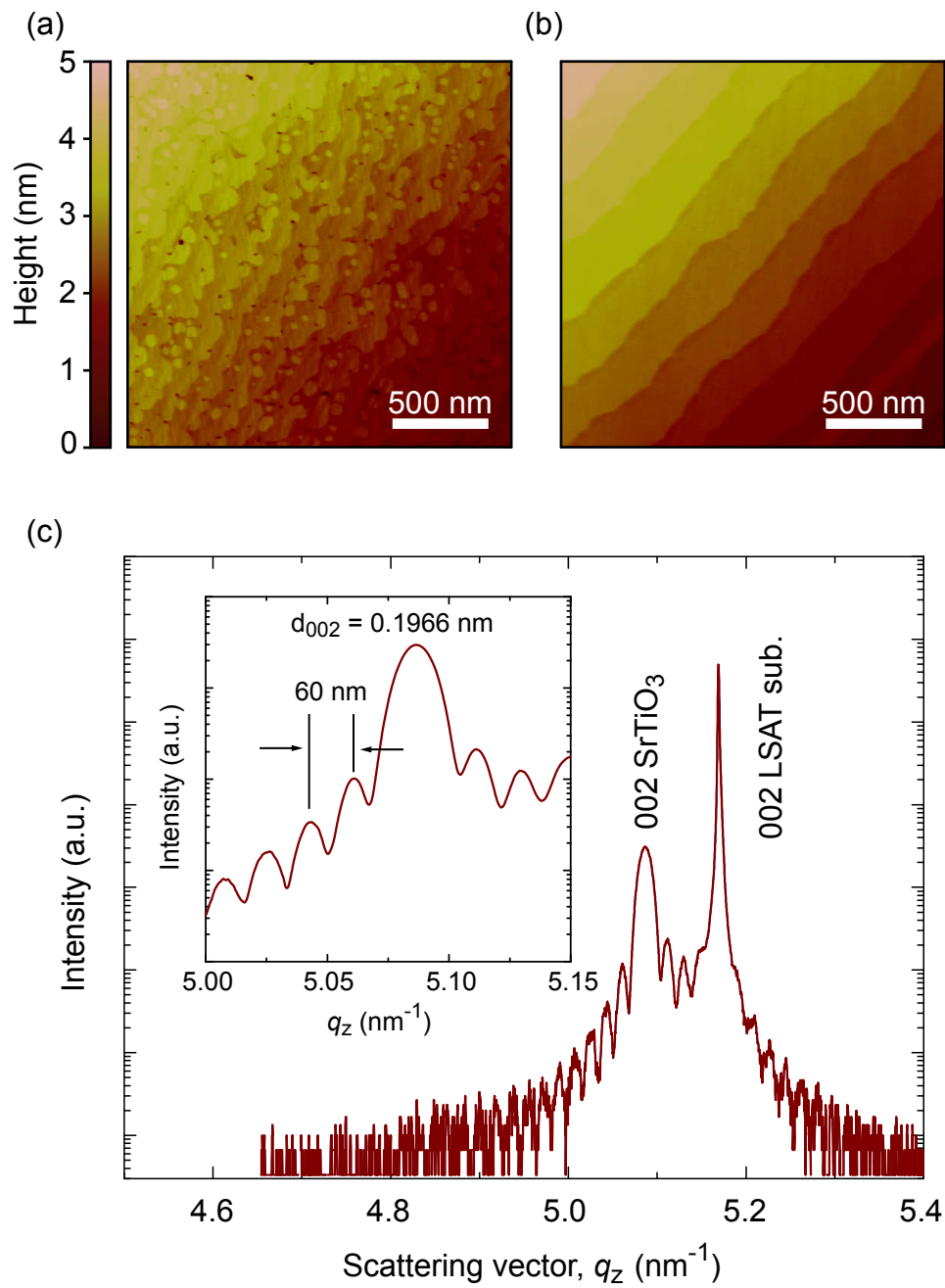


Fig. 1

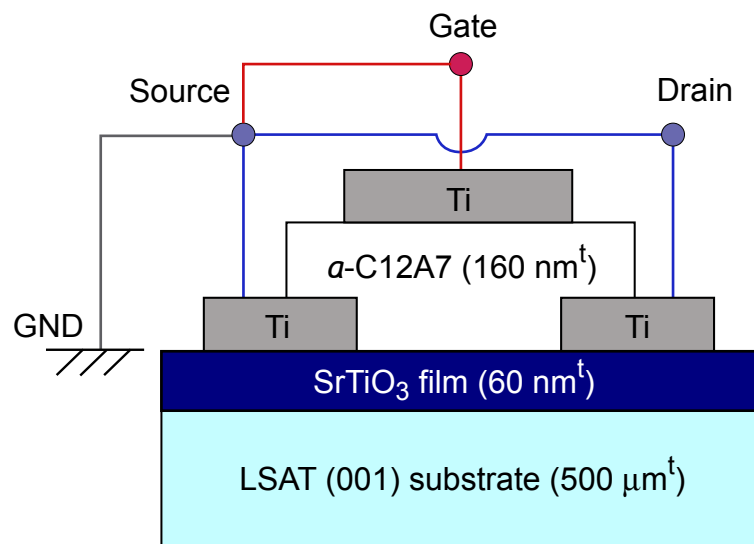


Fig. 2

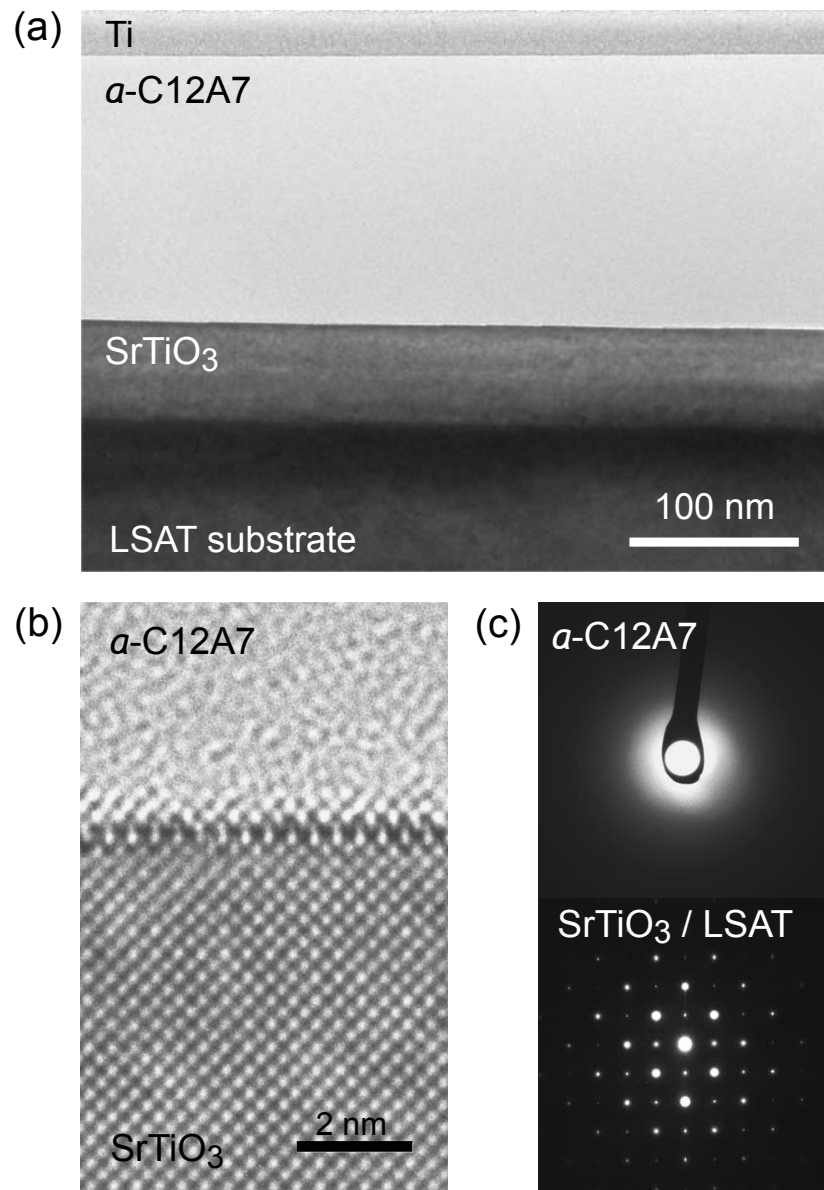


Fig. 3

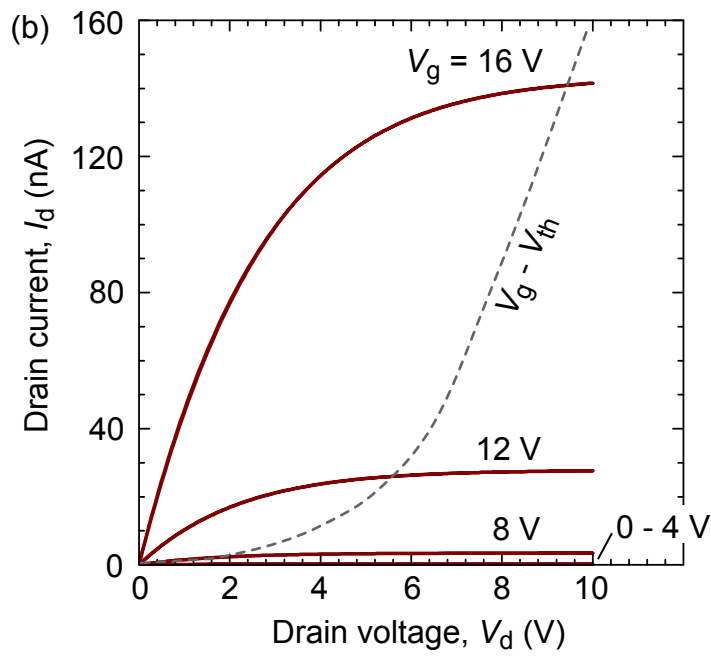
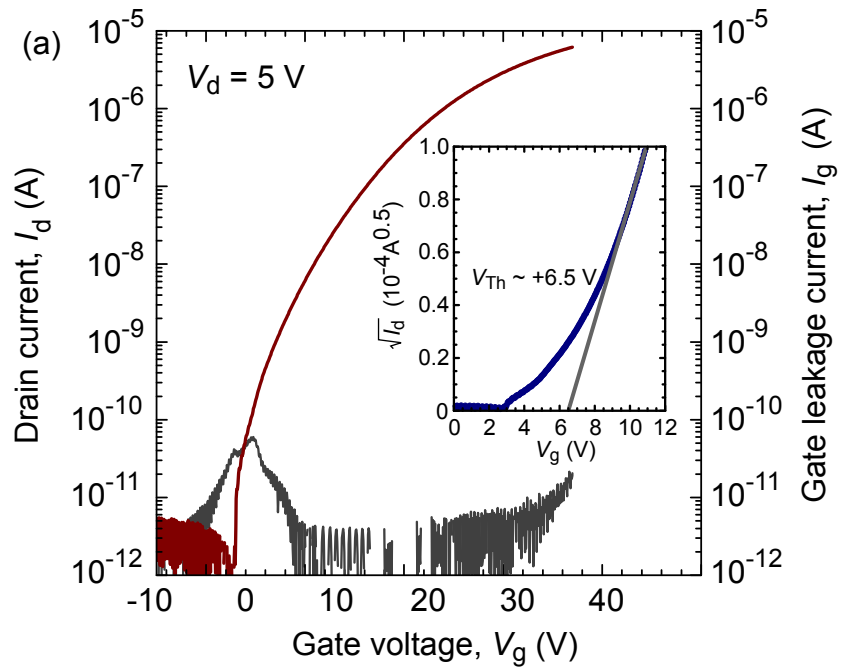


Fig. 4